Charting Microbial Phenotypes in Multiplex Nanoliter Batch Bioreactors

ARTICLE *in* ANALYTICAL CHEMISTRY · APRIL 2013

Impact Factor: 5.64 · DOI: 10.1021/ac400648z

analytical chemistry

Article

pubs.acs.org/ac

Charting Microbial Phenotypes in Multiplex Nanoliter Batch Bioreactors

Jing Dai,[†,⊗] Sung Ho Yoon,[‡,⊗] Hye Young Sim,[†] Yoon Sun Yang,[†,⊥] Tae Kwang Oh,[*,‡,§] Jihyun F. Kim,[*,‡,∥] and Jong Wook Hong[*,†]

[†]Materials Research and Education Center, Department of Mechanical Engineering, Auburn University, Auburn, Alabama 36849, United States

[‡]Systems and Synthetic Biology Research Center, Korea Research Institute of Bioscience and Biotechnology, Daejeon 305-806, Korea

[§]21C Frontier Microbial Genomics and Applications Center, Korea Research Institute of Bioscience and Biotechnology, Daejeon 305-806, Korea

[∥]Department of Systems Biology, Yonsei University, Seoul 120-749, Korea

Supporting Information

ABSTRACT: High-throughput growth phenotyping is receiving great attention for establishing the genotype−phenotype map of sequenced organisms owing to the ready availability of complete genome sequences. To date, microbial growth phenotypes have been investigated mostly by the conventional method of batch cultivation using test tubes, Erlenmeyer flasks, or the recently available microwell plates. However, the current batch cultivation methods are time- and labor-intensive and often fail to consider sophisticated environmental changes. The implementation of batch cultures at the nanoliter scale has been difficult because of the quick evaporation of the culture medium inside the reactors. Here, we report a microfluidic system that allows independent cell cultures in evaporation-free multiplex nanoliter reactors under different culture conditions to assess the behavior of cells. The design allows three experimental replicates for each of eight culture environments in a single run. We demonstrate the versatility of the device by performing growth curve experiments with *Escherichia coli* and microbiological assays of antibiotics against the opportunistic pathogen *Pseudomonas aeruginosa*. Our study highlights that the microfluidic system can effectively replace the traditional batch culture methods with nanoliter volumes of bacterial cultivations, and it may be therefore promising for high-throughput growth phenotyping as well as for single-cell analyses.

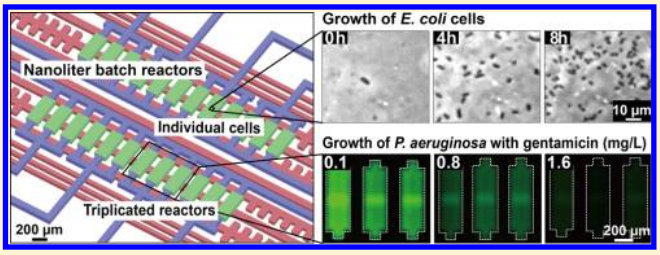

One of the most fundamental challenges in biology is to understand the relationship between a genetic DNA sequence (genotype) and the engendering observable cellular trait (phenotype) in individual cells.[1] Recent advances in high-throughput DNA sequencing technology and molecular measurement techniques allow "omics"-scale analysis of genetic information flow from genome to transcriptome to proteome to metabolome of a microorganism.[2−5] Traditionally, phenotypes have been referred to as characteristics related to cell growth, shape, color of the colonies, formation of biofilms or spores, cell-to-cell interaction, as well as growth pattern.[6] Growth phenotypes are the expression of genotypes and reflect microbial physiology. For example, the growth curve experiments, which are mostly performed in batch cultures, generate primary information such as nutrient utilization profiles and growth kinetics data required for microbial taxonomy and genetic analysis. In addition, this information is widely used in systems biology to measure the impact of environmental and genetic perturbations on complex networks.[2,7−9] Consequently, a great deal of effort has been directed toward the development of novel high-throughput quantitative techniques for microbial growth assessment.[10−13]

Conventional batch culture techniques for studying cell physiology and developing bioproducts remain unchanged for centuries and are still in use by most of the academic biology laboratories and the biotechnology industry. They require a number of test tubes, Erlenmeyer flasks, or agar plates consuming large amounts of media and laborious manual procedures of optical density measurements or microscopic observations. To overcome these challenges, a commercial system has been made to test microbial strains on a 96-well plate, which requires expensive and large instrumentation. Indeed, it is not ideal for automation and miniaturization.[2,6,14] Consequently, efforts have been directed toward the application of microtiter plates to small-scale (submilliliter) bioreactors for batch and fed-batch cultivation, by improving the control over

Received: March 1, 2013
Accepted: April 15, 2013

   dx.doi.org/10.1021/ac400648z | *Anal. Chem.* XXXX, XXX, XXX−XXX

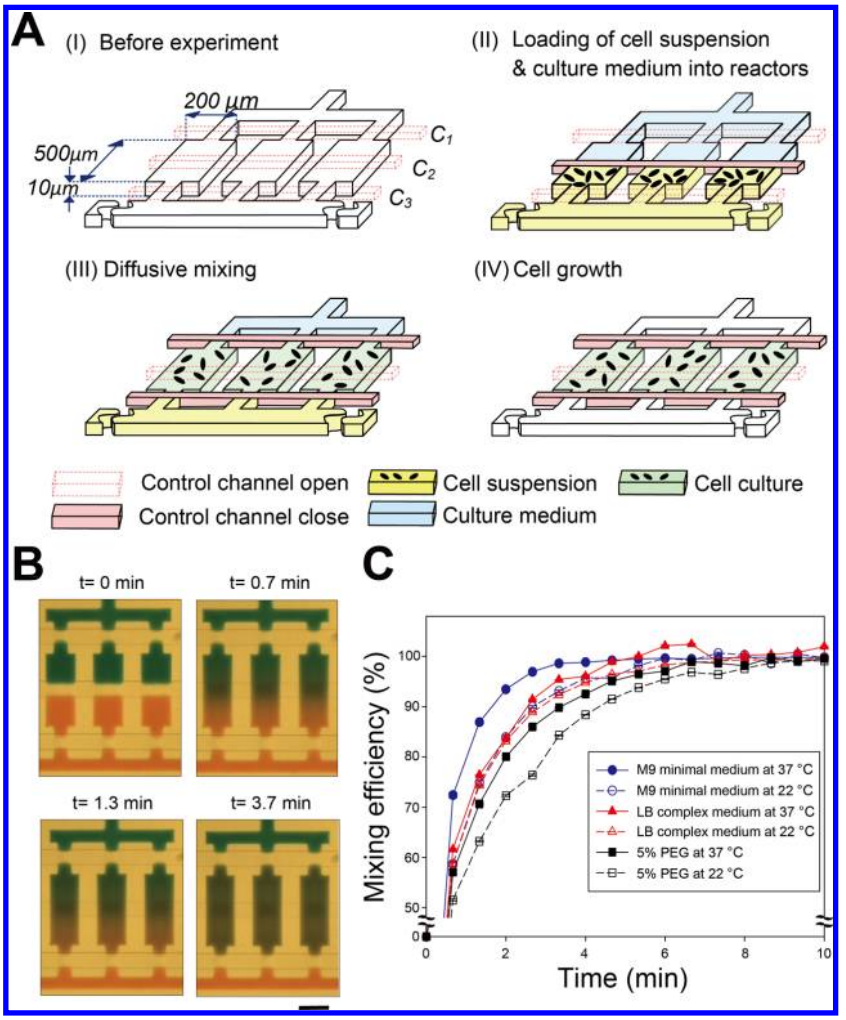

Figure 1. Operation of the device. (A) Schematic drawing of the entrapment of cells into three replicate cultivation reactors (I). The middle control channel C2 is closed to load cell suspension (shown in yellow) and culture media (shown in light blue) into the reactors (II). Cells and the medium are mixed by opening C1 and closing both C1 and C3 (III). The cell cultures are sequestered from the fluid channels, and the cells start to grow (IV). Simultaneous triplicate experiments for testing a culture condition can be performed in a single run. Note that control channels and flow channels are at different layers (see Figure S1 in Supporting Information for details). (B) Time-lapse micrographs showing the mixing of green and red dyes in M9 medium at 37 °C. The process of diffusion was initiated by opening C2 and was almost completed in 4 min. Scale bar, 200 μm. (C) A graph representing the time profiles of mixing efficiency of two dyes dissolved in M9 minimal medium, LB complex medium, and 5% PEG solution at 22 or 37 °C. Error bar denotes the standard error of the mean from three replicate reactors.

culture parameters such as temperature, dissolved oxygen, pH, and medium composition.[10,15−17]

Recent developments in microfluidics provide highly multiplex and quantitative measurements of individual cells, which replace the conventional liquid culture methods with economical and versatile miniaturized devices.[18−24] The application of soft-lithography technology using elastomers such as polydimethylsiloxane (PDMS) in microfluidics has enabled fabrication of micro- or nanostructures such as valves, pumps, chambers, and channels in microfluidic cell culture systems.[18,20,25,26] The microfluidics-based bioreactors offer several advantages over flask cultures or multiwell plates, including precise control of growth conditions and manipulation of nano- or picoliter volumes of culture media, capacity to integrate real-time growth and image measurements, ease of automation, ability to perform a large number of growth experiments under different conditions at the same time, and cultivation at the single-cell level.

Most of the microfluidic cell culture systems reported to date operate in semicontinuous[27] or continuous culture[17,23,24,28,29] modes, so-called microchemostat, where a continuous exchange of fresh medium with the same component occurs through a multitude of growth chambers. However, practically, the functionality of any proposed microchemostat differs in cells cultured in a batch process. Long-term culturing in microchemostats inevitably leads to the formation of biofilm, which poses a significant problem in nanoliter-scale bioreactors with a high surface-to-volume ratio.[27] In addition to the presence of a high risk of contamination due to intermittent cleaning of the reactor surfaces, the microchemostat devices often utilize a single growth medium, which is insufficient for testing multiple growth environments. Besides, in most of the laboratories, a large number of cell culture processes are operated in batch mode as it generates important growth kinetics data required for taxonomic identification, genetic-phenotypic analysis, and systems modeling purposes.[6] This necessitates the development of a multiplex microfluidic culture system that simulates macrocultures, which have been mainly performed in flasks, tubes, or microtiter plates.

dx.doi.org/10.1021/ac400648z | Anal. Chem. XXXX, XXX, XXX−XXX

Despite its importance in microbial taxonomy, genetic-phenotypic analysis, and systems biology, a batch culture process on the nanoliter scale has rarely been realized. This is primary due to that PDMS is permeable to water vapor and the culture medium inside a PDMS nanoliter reactor is easily evaporated, leading to complete drying over time.[20,30] Also, implementation of on-chip mixing requires more operational steps, further complicating the system. Recently, a microfluidic batch chip was developed to have 120 culture reactors (50 nL each) in which the cell suspension was circulated and the whole chip was put in a water bath for temperature and humidity control.[21] However, the active mixing by circulation of the cell suspension mimicked the previous microchemostats, which makes the platform difficult to test multiple culture conditions without changing the reactor design.

In the present study, we devised a multiplexed microfluidic batch culture chip that enables microbial growth in 24 sets of discrete bioreactors (1 nL each), while simultaneously allowing the assessment of eight different culture conditions in parallel. The flow channels and culture reactors were designed to maintain a uniform distribution of cells in each reactor and to conduct experiments in triplicates in a single run. The evaporation of the cell culture medium present in each of the batch reactors was overcome by placing the chip in a humidified incubator and incorporating antievaporation channels around the reactor within the chip. Further, we demonstrate the utility of our system in characterizing microbial growth phenotypes by monitoring the growth of *Escherichia coli* with different carbon sources, obtained by both chip and tube cultures. We also show that the system could be successfully integrated with a fluorescence detection device for real-time observation of cell growth via online monitoring of fluorescent reporters of the opportunistic pathogen *Pseudomonas aeruginosa* incubated under different antibiotic concentrations.

EXPERIMENTAL SECTION

Chip Fabrication. The platform employed in the present study was fabricated by standard multilayer soft lithography.[25,31,32] The mask was designed using AutoCAD software (AutoDesk Inc., San Rafael, CA), which was printed on a transparent film at 20 000 dpi (CAD/Art Services, Inc., Bandon, OR). Molds for the two layers, fluidic and control layers, were prepared by a photolithographic technique using a positive photoresistor (AZ P4620; AZ electronic materials, Branchburg, NJ) onto a 4-in. silicon wafer. This was followed by UV exposure and development. To facilitate reliable opening and closing of the valves, the photoresistor for fluidic layer was rounded by heating the mold at 130 °C for 2 min. We fabricated the top thick fluidic layer of the chip by pouring uncured PDMS (RTV615; Momentive Performance Materials, Waterford, NY; elastomer/cross-linker = 10:1) onto the fluidic layer mold to achieve a thickness of 5 mm. Then, the bottom control layer of the chip was fabricated by spin-coating uncured PDMS (elastomer/cross-linker = 20:1) onto the control layer mold at 3000 rpm for 1 min. Subsequently, the fluidic layer and control layer were cured at 80 °C for 1 h and 45 min, respectively. Thereafter, the fluidic layer was peeled off from the mold, and holes for inlet and outlet ports to flow channels through the thick layer were created using a 19-gauge punch (Technical Innovations, Inc., Brazoria, TX). The fluidic and control layers were aligned and bonded by baking at 80 °C for 80 min, followed by punching holes for inlets to the control channels. The resulting PDMS chip was placed on a precleaned glass slide (Fisher Scientific, Pittsburgh, PA) and cured by incubating in an oven at 80 °C for 18 h.

Loading of Fluorescent Beads or Bacterial Cells in Nanoliter Reactors. Fluorescent beads (diameter, 2.0 μm; concentration, 2.84×10^8 particles/mL) or bacterial cells were loaded through "cell in" channels by applying 34 kPa loading pressure. By opening the C1 and C3 control channels (Figure 1A), beads or cells were loaded into 12 nanoliter reactors. After maintaining the loading pressure for 1 min, the C1 and C3 channels were closed to retain beads or cells in the nanoliter reactors.

Bacterial Strains. *E. coli* K12 (ATCC 25404) and its lactose nonfermenting (*lac*$^-$) mutant (AB3568, F-, Δ(*cod-lacI)6*, *rpsL60*(strR))[33] were purchased from the American Type Culture Collection (Manassas, VA) and The Coli Genetic Stock Center (New Haven, CT), respectively. *P. aeruginosa* PT5 was a gift from Dr. Thilo Köhler. The pE21-EGFP vector having a GFP mutant gene was donated by Dr. Moonil Kim. The GFP, which is a red-shift mutation of the wild GFP, has an excitation wavelength of 488 nm and an emission wavelength of 507 nm. pE21-EGFP was transformed into PT5 to construct the PT5-EGFP strain, according to the standard transformation protocol.[34]

Cultivation of *E. coli* in Tubes and Nanoliter Reactors. A seed culture was prepared by growing cells in a 14-mL test tube containing 4 mL of LB medium, placed in a incubator with shaking 160 rpm at 37 °C overnight (1.0−1.4 at OD_{600}). For cell growth in a tube, the seed culture was diluted with fresh LB medium to obtain an OD_{600} of 0.01. A volume of 4 mL of the cell inoculum was aerobically grown in a 14-mL tube at 37 °C with shaking at 160 rpm. As for *lac*$^-$ mutant, the LB medium was supplemented with 40 μg/mL streptomycin (Sigma-Aldrich, St. Louis, MO). For cell growth in a nanoliter reactor with LB medium, the seed culture was diluted with fresh LB medium to obtain an OD_{600} of 0.1 and was subsequently introduced into a reactor. For cell growth in a reactor with M9 medium, cells from the seed culture were harvested by centrifugation at 7 711*g* for 1 min, washed 3 times with M9 medium, and then suspended with M9 medium to obtain an OD_{600} of 0.1. Thereafter, they were introduced into each of the nanoliter reactors containing M9 medium with different carbon source(s): no carbon source, glucose (0.4% wt/vol), lactose (0.4%), and lactose (0.4%) plus glucose (0.08%). Finally, the chip was incubated at 37 °C in a humidity control system developed in our laboratory.

Cultivation of *P. aeruginosa* Harboring pEGFP in Tubes and Nanoliter Reactors. A seed culture was prepared by growing cells in a 14-mL test tube containing 4 mL of M9 medium supplemented with Casamino Acids (0.5% wt/vol), $MgSO_4$ (1.0 mM), and glucose (11.1 mM), and 100 μg/mL of ampicillin overnight (1.7−1.8 at OD_{600}). Subsequently, the cells were harvested by centrifugation at 1 600*g* for 10 min, washed once with 2× M9 medium, and then suspended in 2× M9 medium to obtain an OD_{600} of 0.2. Various concentrations of gentamicin (Sigma-Aldrich, St. Louis, MO) (0, 0.2, 0.4, 0.8, 1.6, 3.2, 6.4, and 12.8 mg/L) were prepared by diluting 100 mg/L of gentamicin stock solution in water. A volume of 2 mL of gentamicin solution was added to 2 mL of the cell inoculum in a 14-mL tube, and the cells were allowed to grow aerobically at 37 °C with shaking at 160 rpm. For cell growth in a nanoliter reactor, the cell inoculum along with a different concentration of gentamicin was introduced into the reactor. Finally, the chip

dx.doi.org/10.1021/ac400648z | *Anal. Chem.* XXXX, XXX, XXX−XXX

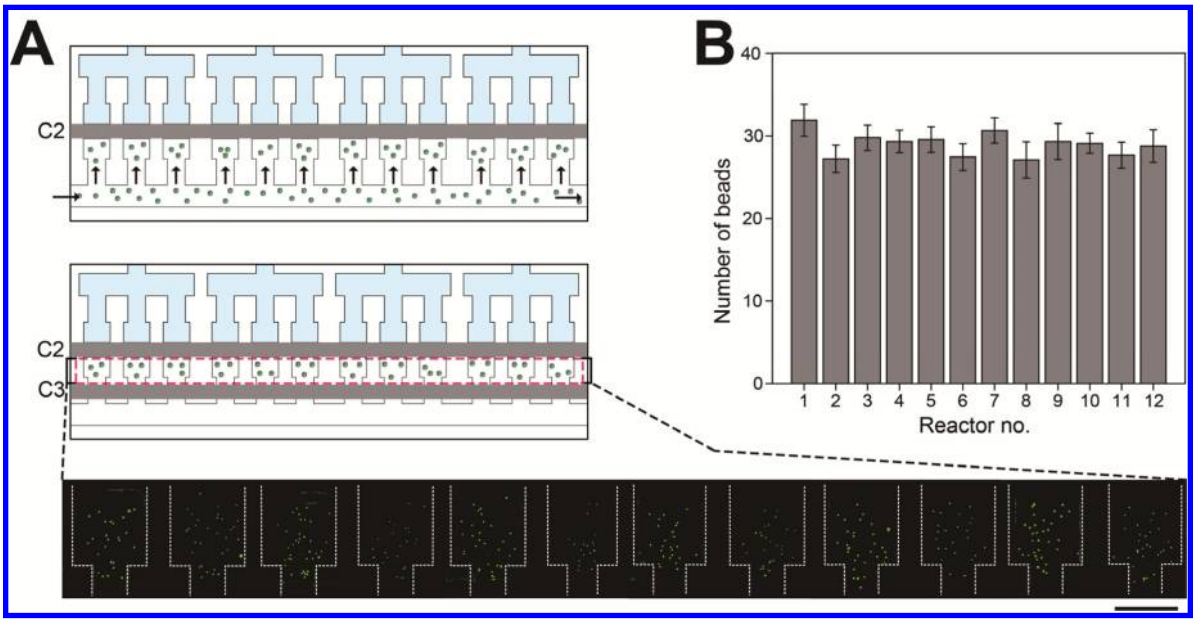

Figure 2. Loading of a uniform number of particles into the reactors. (A) Fluorescent beads (2.0 μm) are loaded into each of the 12 reactors by opening C3 control channel, followed by the closing of C3 channel, which retains the beads. Arrows denote the direction of bead suspension flow. Scale bar, 200 μm. (B) Number of beads loaded into each of the reactors. Error bar denotes the standard error of the mean from nine separate experiments.

was incubated at 37 °C in a humidity control system developed in our laboratory.

Image Acquisition and Data Analysis. The microfluidic chip was analyzed using an inverted optical microscope (Axiovert 40 CFL; Carl Zeiss, Munich, Germany) equipped with a CCD camera (Moticam 1000; Motic, Inc., Richmond, BC, Canada). Bright-field images were captured at 40× magnifications every 2 h and digitized using Motic Images Plus 2.0 software (Motic, Inc., Richmond, BC, Canada). For tube culture of PT5-EGFP, the fluorescence intensity was obtained using a Hitachi F-7000 fluorescence spectrometer (Pleasanton, CA) with 488 ± 10 nm of excitation and 507 ± 10 nm of emission. The fluorescence intensity of 150 μL of PT5-EGFP cells in a 1000-μL cuvette was measured. For cell culture in nanoliter reactors, the fluorescence image was obtained using a modified ArrayWoRx biochip scanner (Applied Precision, Issaquah, WA) with 480 ± 15 nm of excitation and 530 ± 20 nm of emission. The fluorescence images were digitized using ImageJ software (NIH, Bethesda, MD).

Mixing Efficiency of the Reagents Inside the Nanoliter Reactors. We captured the mixing phenomena by using an inverted microscope (Axiovert 40 CFL; Carl Zeiss, Munich, Germany) equipped with a CCD camera (Moticam 1000, Motic, Inc., Richmond, BC, Canada). Time series analyzer of ImageJ software was employed for digitizing the captured images and obtaining the gray value of each reactor. When mixing was complete, the value remained constant. To quantify the mixing efficiency based on the average gray value, we defined an equation as follows:

$$I(\%) = \frac{G_i - G}{G_i - G_f} \times 100\% \quad (1)$$

where I is the mixing efficiency; and G_i, G, and G_f are the average gray values of initial time, given time, and final time, respectively.

Statistical Analyses. The ANOVA test was used to determine the statistical significance of distribution of beads loaded per bioreactor. Normality and constant variance assumption were checked by using Anderson-Darling and Levene's tests, respectively (MINITAB 14, Minitab Inc., State College, PA). The bootstrapping method in the R statistical package was used to assess the significance of the correlation between cell densities and log-transformed antibiotic concentrations.

RESULTS AND DISCUSSION

Design and Operation of the Multiplex Microfluidic Nanoliter Device. The PDMS device features a 20-μm thin control layer that is overlaid with a 5-mm thick fluidic layer, which is placed on a glass slide (Figure S1A in the Supporting Information). The fluidic layer has two parallel rows of 12 culture reactors, each with a volume of 1 nL (Figure S1B in the Supporting Information). Each row is connected to a single-cell suspension channel and four different medium channels, where each of them correspond to three culture reactors. This design enables simultaneous triplicate experiments for each of the eight culture environments in a single run.

Cell suspension and fresh medium were loaded into three reactors present as a single unit, by opening two control channels located at the ends of the reactors (C1 and C3 in Figure 1A) and closing a control channel at the middle of the reactors (C2). Once they were filled into each half of the reactor, the modes of the channels were switched to open C2 and to close C1 and C3, causing diffusive mixing of the cells and the medium. The diffusion efficiency was determined by monitoring the mixing of green and red dyes (ESCO Foods, Inc., San Francisco, CA) dissolved in M9 medium, Luria–Bertani (LB) complex medium, or 5% polyethylene glycol (PEG) solution (Figure 1B,C; Supporting Video S1 in the Supporting Information). We observed approximately 33–55% increase in the mixing efficiency, when the temperature was increased from 22 to 37 °C. The mixing efficiency decreased with the increase in the viscosity of the medium (viscosity: M9 < LB < 5% PEG). All the tested media showed complete mixing

dx.doi.org/10.1021/ac400648z | Anal. Chem. XXXX, XXX, XXX–XXX

in approximately 9 min, which is negligible when compared to the time taken for the generation of microbial cells in growth curve experiments (for example, at least 12 h for the fast-growing *E. coli*).

Uniform Distribution of Particles Loaded Per Bioreactor. The flow of cell-suspension channel perpendicular to the reactors caused the fluid to be pumped tangentially along the entrance of each of the reactors (Figure 2A). Distribution of particles confined in the reactors was analyzed using 2.0-μm fluorescent polystyrene beads (Polysciences, Inc., Warrington, PA, USA). An applied pressure of 34 kPa to the suspension flow forced a portion of the fluid into the reactors. No build-up of the beads was observed at the entrances of the reactors, and hence, closing of the entrances led to the retention of the particles in the reactors, which thus resulted in the uniform distribution of beads trapped in the reactors (29 ± 2 beads per reactor, *P*-value =0.713) (Figure 2B). Thus, loading of a nearly constant number of cells into each of the reactors allows direct and unbiased comparison of growth phenotypes from the reactors.

Evaporation-Free Batch Cultivation. A major challenge in employing microfluidic PDMS devices for cell cultivation at the nanoliter scale is that PDMS, being permeable to water vapor, results in rapid evaporation of the culture medium inside the microfluidic chambers.[20,30] Evaporation is a matter of great concern in batch cultivation, where the initially supplied liquid medium is not sufficient to support cell growth for a long-term culture. In contrast, this issue can be avoided by the use of fed-batch[27] or continuous[17,28,29] cultures through continuous renewal of the medium. In this study, we resolved this problem by placing the whole device in a humidified incubator and incorporating water-filled antievaporation channels around the nanoliter reactors within the device (Figure S1B in Supporting Information). Water-filled channels installed around or above reactors can suppress evaporation by letting water to saturate surrounding PDMS.[35,36] The use of water jackets for long-term cultivation could raise a concern of different salt concentrations as the culture chambers. However, as long as the medium in each chamber is retained to be constant during the culture, the variation in the medium concentration should be negligible.

To determine the effects of antievaporation channels and humidified incubator on the degree of evaporation of the media inside the reactors, we measured the amount of green dye that was retained in the reactors at 37 °C after 24 h (Figure 3; Figure S2 in Supporting Information). Notably, during the initial stage, when the antievaporation channels and the humidified incubator were not operated, evaporation of the medium was observed, which resulted in 7% of volume loss in 4 h to ~26% in 12 h. Further, intensive drying was observed in the middle of the reactors, possibly due to the location of the control channel (C2) and a shorter diffusion path of the membrane thereby (Figure S2 in Supporting Information). Operating antievaporation channels under a pressure of 103 kPa retarded evaporation for 8 h. Furthermore, it was noted that placing the device in a humidity-saturated incubator led to approximately a 2% volume loss in 24 h. That loss seems to be negligible and to be caused by the diffusion through a thin membrane (~10 μm thick) between a reactor chamber and a control channel. However, even relatively small shifts in the osmolality of culture media by evaporation through PDMS can drastically affect sensitive mammalian cell behavior.[37] In addition, when the system is applied to slowly growing cells such as myxobacteria (e.g., *Sorangium cellulosum* with a doubling time of 16 h),[38] the adverse effect caused by the volume change can be profound. Strikingly, by operating antievaporation channels along with use of the humidified incubator, virtually 100% of the initial volume in the reactors was maintained throughout incubation. Therefore, our finding highlights the importance of conditioning microfluidic devices in humidified environment in preventing evaporation and further demonstrates that a continuous supply of water molecules from the antievaporation channels contributes to the saturation of PDMS backbone-pores around the reactors.

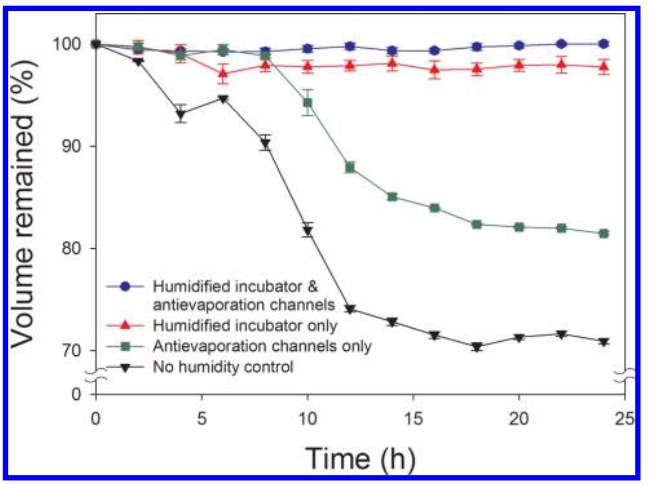

Figure 3. Effect of humidity controls on volume changes of the medium inside the reactors. The graph represents the volume changes of the initial medium over a period of time (24 h duration) based on the presence and/or absence of humidity control and/or antievaporation channels: in the absence of humidified incubator (denoted with a black line), in the presence of operation of antievaporation channels (green line), in the presence of a humidified incubator (red line), and in the presence of both humidified incubator and the operation of antievaporation channels (blue line). The error bar denotes the standard error of the mean, obtained from three replicate reactors.

Application of the Device to Measure Bacterial Growth Phenotypes. As denoted above, we succeeded in developing a novel microfluidic batch culture system that enables uniform distribution of cells in each bioreactor and aids in evaporation-free cultivation for a long-term, which have been the major challenges in the development of PDMS-based microculture devices for batch cultivation. Cultivation-associated physiological environment can be easily changed when the reactor volume changes from macro- to microscale.[20,39] Therefore, we investigated whether the designed system would allow sensitive and accurate measurements of bacterial growth phenotypes equivalent to the traditional methods, by performing growth curve experiments with *Escherichia coli* and microbiological assays of antibiotics against the opportunistic pathogen *Pseudomonas aeruginosa*.

Growth Curve Experiments. We demonstrated the utility of the developed device to replace the traditional methods by performing batch cultivation using one of the most commonly used laboratory strains of *E. coli* K-12. We obtained micrographs of the cells grown on the LB complex medium every 2 h after inoculation and counted the number of cells (Figure 4A). The growth curves were compared with the results obtained from the batch cultures of *E. coli* grown in 14-mL tubes, each containing 4 mL of LB medium (Figure 4B). The growth profiles derived from both methods reflected the typical batch growth curve of *E. coli*, and were highly similar to each

dx.doi.org/10.1021/ac400648z | Anal. Chem. XXXX, XXX, XXX–XXX

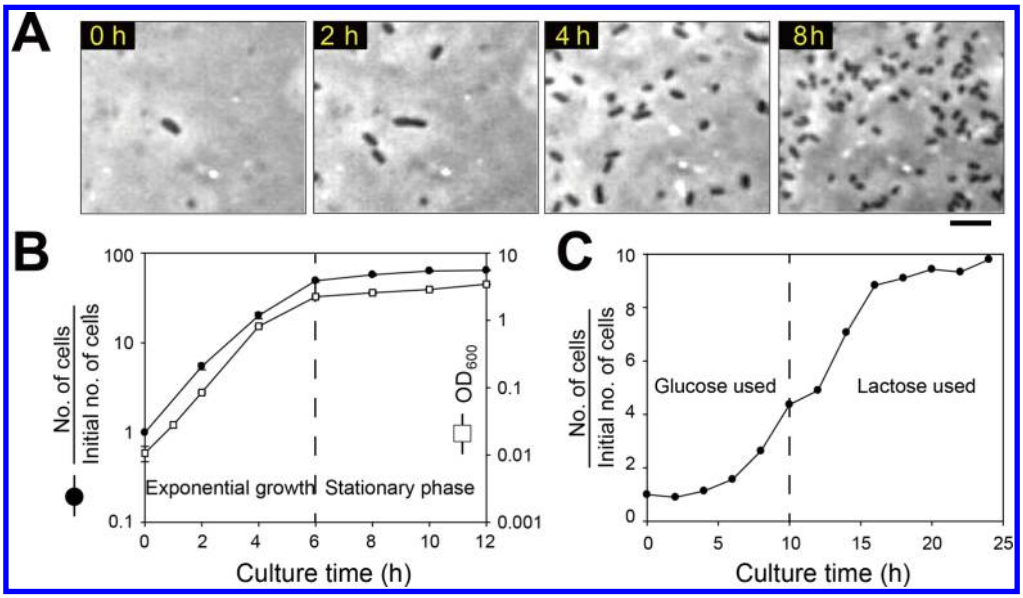

Figure 4. Growth of *E. coli* cells during batch culture in a nanoliter reactor. (A) Micrographs showing time-lapse cell growth on the LB complex medium in a nanoliter reactor. Scale bar, 10 μm. (B) A graph showing the comparison of cell growth on LB medium in the nanoliter reactor (represented by ●) with that in a 14-mL test tube containing 4 mL of LB medium (□). The cell numbers in the reactors were counted every 2 h after inoculation and were normalized to the initial number of cells. The cell density in a tube culture was measured in OD_{600}. Values on the *Y* axes are in log scale. Error bar denotes the standard error of the mean from three replicate reactors or test tubes. (C) A graph showing the diauxic growth on M9 minimal medium with glucose (0.04% wt/vol) and lactose (0.2%) in a nanoliter reactor.

other. When grown in M9 minimal medium with glucose (0.04% wt/vol) and lactose (0.2%) as carbon sources, nanoliter reactors reproduced the famous diauxic growth curve,[40] characterized by two exponential phases separated by a lag period during which cells produce enzymes required to metabolize the less-preferred carbon source (Figure 4C). Furthermore, we assessed the growth patterns of a known mutant with different carbon sources, in order to determine the ability of the device in accurately characterizing mutant phenotypes (Figure S3 in the Supporting Information). Notably, lactose nonfermenting (lac^-) mutant of *E. coli* K12[33] failed to grow on lactose as a sole carbon source and did not show the diauxic growth pattern when grown on glucose and lactose as it lacked the lactose-metabolizing capability.

Microbiological Assay for Antibiotics. We validated the capability of the device in determining the concentration-dependent antibacterial activity of gentamicin against the opportunistic pathogen *P. aeruginosa*, which is responsible for nosocomial infections such as severe ventilator-associated pneumonia and bacteremia.[41] For real-time measurement of the cell growth, we employed a fluorescence-based scanner to capture and quantify fluorescence intensity of the growing cells. For this purpose, we employed *P. aeruginosa* that constitutively expressed plasmid-encoded enhanced green fluorescent protein (pEGFP). The pEGFP was reported to be stable for long-term bacterial cultures, without interfering with cell growth.[42] Fluorescence intensity and the cell number in the bioreactors were measured by employing a modified biochip scanner, following visual inspection using a microscope. We observed that there was a significant linear correlation (R^2 = 0.986) between fluorescence signal and the cell density (Figure S4 in the Supporting Information). Strikingly, in such a small culture volume (1 nL), cells were diffusively mixed and reached reasonably homogeneous growth conditions (Figure S5 in the Supporting Information; see Figure 4A for *E. coli* cultivation). Most of microbioreactor systems reported to date use active mixing components for microbial culture to ensure homogeneous conditions,[21,27,43,44] which requires delicate and complicated steps for the fabrication and operation of such devices. In this regard, homogeneous conditions achieved by diffusive mixing in our system can contribute to the development of high-throughput microfluidic devices for phenotypic analysis.

Further, we measured and compared the concentration-dependent inhibitory effects of gentamicin on *P. aeruginosa* harboring the EGFP plasmid, in the cultures obtained from both nanoliter reactors and test tubes (Figure 5; Figure S5 in Supporting Information). In the case of test tube cultures, at 24 h following inoculation, the cell density was found to be inversely correlated significantly with log-transformed antibiotic concentration (r = −0.98, P-value ≈ 0), which is in accordance with previous observations.[45,46] Remarkably, similar results were obtained using cultures from nanoliter reactors (r = −0.87, P-value < 0.007), indicating that our developed system could be employed for microbiological assay of antibiotics. The slight different inhibitory effects in the microfluidic cultures from those in the 14 mL test tube cultures might be a result of higher cell density (Figure 5) or diffusion dependent cell behavior in microenvironments.[39,47,48]

■ CONCLUSIONS

We demonstrated the utility of the device in charting phenotypic changes of *E. coli* by assessing the growth patterns with different carbon sources and also of *P. aeruginosa* cells in response to growth inhibitors with various concentrations of antibiotics through fluorescence-based growth measurement. Our system was designed to conduct experiments in triplicate in a single run and ensure uniform distribution of cells in nanoliter reactors at the inoculation stage, which enabled direct comparison of the results from eight different culture environments. Importantly, virtually complete prevention of

dx.doi.org/10.1021/ac400648z | *Anal. Chem.* XXXX, XXX, XXX−XXX

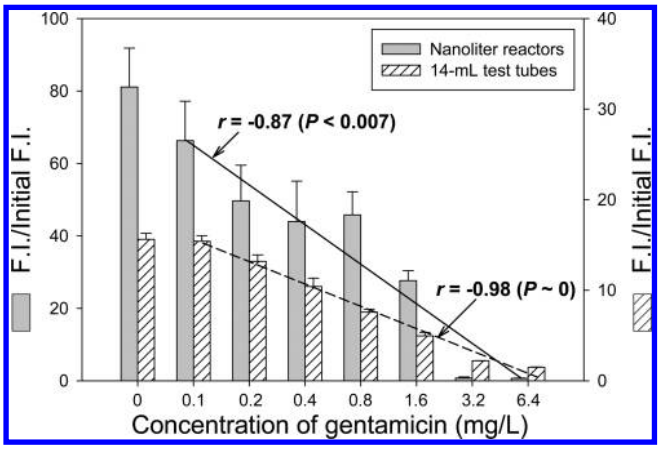

Figure 5. Microbiological assay for antibiotics using a nanoliter reactor and a test tube. The graph shows the comparison of antibiotic effects of gentamicin on the growth of *P. aeruginosa* harboring the EGFP plasmid, following 24 h of culture in nanoliter reactors (represented using gray bars, on the left side), with that in the 14-mL test tubes (represented using hatched bars, on the right side). The *X* axis denotes concentration of gentamicin in log scale, and the *Y* axis denotes the fluorescence intensity (F.I.) normalized to the initial intensity of the cell culture, immediately following inoculation. The error bar represents the standard error of the mean from three replicate reactors or test tubes.

evaporation of the cell culture media was achieved by placing the device in a humidified incubator and installing water-filled antievaporation channels around the nanoliter reactors within the device. The present device has a simple architecture, ease of operation, and ability to precisely control multiple culture conditions while the batch culture format simulates a conventional microbial assay. This could further be exploited for investigating host–microbe interactions and applied to a variety of cell types, not limited only to bacteria. In addition, by increasing the number of reactors and adding a concentration gradient generator at the inlets of the reactors, the device could be used to screen a multitude of metabolites, peptides, and proteins, thereby significantly reducing time and expenditure involved in drug-screening processes. Collectively, our study confirmed that high-throughput growth phenotyping using multiplex nanoliter batch reactors, in combination with real-time growth and image measurements, will meet the increasing demand for genome-wide studies, single cell analyses, as well as drug discovery.

■ ASSOCIATED CONTENT

Ⓢ Supporting Information

(Figure S1) Design of the multiplex microfluidic nanoliter chip; (Figure S2) micrographs showing time profiles corresponding to the amount of green dye, which was retained in the reactors at 37 °C, based on the presence and/or absence of humidity control and/or antievaporation channels; (Figure S3) graph showing the time profile corresponding to the number of *lac*$^-$ *E. coli* mutants, which was normalized to the initial number of cells; (Figure S4) graph showing the correlation between cell density and fluorescence intensity of PT5-EGFP; (Figure S5) concentration-dependent inhibitory effect of gentamicin on PT5-EGFP strain; and (Supporting Video S1) mixing of green and red dyes dissolved in M9 medium at 37 °C in the bioreactors. This material is available free of charge via the Internet at http://pubs.acs.org.

■ AUTHOR INFORMATION

Corresponding Author

*E-mail: hongjon@auburn.edu (J.W.H.); jfk1@yonsei.ac.kr (J.F.K.); otk@kribb.re.kr (T.K.O.).

Present Address

⊥Y.S.Y.: Department of Medical Cell BioPhysics (MCBP), MIRA Research Institute, University of Twente, Enschede, The Netherlands.

Author Contributions

⊗J.D. and S.H.Y. contributed equally to this work.

Notes

The authors declare no competing financial interest.

■ ACKNOWLEDGMENTS

The authors are grateful to Dr. Thilo Köhler at University of Geneva, Switzerland, for kindly providing us with *P. aeruginosa* PT5; Moonil Kim for providing pE21-EGFP vector; Jae Young Yun for helping in image analysis; Sachin Jambovane and Morgan Hamon for helpful comments and heartful support. This work was supported by the Korean Ministry of Education, Science and Technology through the 21st Century Frontier R&D Program of Microbial Genomics and Applications Center (to J.F.K and J.W.H.) and the Global Frontier Intelligent Synthetic Biology Center (Grant NRF-2012M3A6A8053632 to J.F.K. and 2011-0031952 to S.H.Y.). The work of J.W.H. was also supported by the U.S. National Institute of Health (NIH Grant R01 EB008392) and the USDA Nanotechnology Program (CSREES Grant No. 2008-01437). Financial support also came in part from the National Research Foundation (Grants NRF-2011-0017670 and 2012-0001151 to J.F.K.) and the Technology Development Program to solve Climate Changes on Systems Metabolic Engineering for Biorefineries (Grant NRF-2012-C1AAA001-2012M1A2A2026559 to S.H.Y.).

■ REFERENCES

(1) Bochner, B. R. *Nat. Rev. Genet.* **2003**, *4*, 309–314.

(2) Yoon, S. H.; Han, M. J.; Jeong, H.; Lee, C. H.; Xia, X. X.; Lee, D. H.; Shim, J. H.; Lee, S. Y.; Oh, T. K.; Kim, J. F. *Genome Biol.* **2012**, *13*, R37.

(3) Schneider, M. V.; Orchard, S. *Methods Mol. Biol.* **2011**, *719*, 3–30.

(4) Lee, S. Y.; Lee, D. Y.; Kim, T. Y. *Trends Biotechnol.* **2005**, *23*, 349–358.

(5) Buescher, J. M.; Liebermeister, W.; Jules, M.; Uhr, M.; Muntel, J.; Botella, E.; Hessling, B.; Kleijn, R. J.; Le Chat, L.; Lecointe, F.; Mader, U.; Nicolas, P.; Piersma, S.; Rugheimer, F.; Becher, D.; Bessieres, P.; Bidnenko, E.; Denham, E. L.; Dervyn, E.; Devine, K. M.; Doherty, G.; Drulhe, S.; Felicori, L.; Fogg, M. J.; Goelzer, A.; Hansen, A.; Harwood, C. R.; Hecker, M.; Hubner, S.; Hultschig, C.; Jarmer, H.; Klipp, E.; Leduc, A.; Lewis, P.; Molina, F.; Noirot, P.; Peres, S.; Pigeonneau, N.; Pohl, S.; Rasmussen, S.; Rinn, B.; Schaffer, M.; Schnidder, J.; Schwikowski, B.; Van Dijl, J. M.; Veiga, P.; Walsh, S.; Wilkinson, A. J.; Stelling, J.; Aymerich, S.; Sauer, U. *Science* **2012**, *335*, 1099–1103.

(6) Bochner, B. R. *FEMS Microbiol. Rev.* **2009**, *33*, 191–205.

(7) Karr, J. R.; Sanghvi, J. C.; Macklin, D. N.; Gutschow, M. V.; Jacobs, J. M.; Bolival, B.; Assad-Garcia, N.; Glass, J. I.; Covert, M. W. *Cell* **2012**, *150*, 389–401.

(8) Covert, M. W.; Knight, E. M.; Reed, J. L.; Herrgard, M. J.; Palsson, B. O. *Nature* **2004**, *429*, 92–96.

(9) Yoon, S. H.; Reiss, D. J.; Bare, J. C.; Tenenbaum, D.; Pan, M.; Slagel, J.; Moritz, R. L.; Lim, S.; Hackett, M.; Menon, A. L.; Adams, M. W.; Barnebey, A.; Yannone, S. M.; Leigh, J. A.; Baliga, N. S. *Genome Res.* **2011**, *21*, 1892–1904.

(10) Duetz, W. A. *Trends Microbiol.* **2007**, *15*, 469−475.
(11) Kumar, S.; Wittmann, C.; Heinzle, E. *Biotechnol. Lett.* **2004**, *26*, 1−10.
(12) Marques, M. P.; Cabral, J. M.; Fernandes, P. *Recent Pat. Biotechnol.* **2009**, *3*, 124−140.
(13) Li, N.; Tourovskaia, A.; Folch, A. *Crit. Rev. Biomed. Eng.* **2003**, *31*, 423−488.
(14) Bochner, B. R.; Gadzinski, P.; Panomitros, E. *Genome Res.* **2001**, *11*, 1246−1255.
(15) Funke, M.; Buchenauer, A.; Mokwa, W.; Kluge, S.; Hein, L.; Muller, C.; Kensy, F.; Buchs, J. *Microb. Cell. Fact.* **2010**, *9*, 86.
(16) Kensy, F.; Engelbrecht, C.; Buchs, J. *Microb. Cell. Fact.* **2009**, *8*, 68.
(17) Zhang, Z.; Boccazzi, P.; Choi, H. G.; Perozziello, G.; Sinskey, A. J.; Jensen, K. F. *Lab Chip* **2006**, *6*, 906−913.
(18) Weibel, D. B.; Diluzio, W. R.; Whitesides, G. M. *Nat. Rev. Microbiol.* **2007**, *5*, 209−218.
(19) Yeo, L. Y.; Chang, H. C.; Chan, P. P.; Friend, J. R. *Small* **2011**, *7*, 12−48.
(20) Velve-Casquillas, G.; Le Berre, M.; Piel, M.; Tran, P. T. *Nano Today* **2010**, *5*, 28−47.
(21) Gan, M.; Tang, Y.; Shu, Y.; Wu, H.; Chen, L. *Small* **2012**, *8*, 863−867.
(22) Dai, W.; Zheng, Y.; Luo, K. Q.; Wu, H. *Biomicrofluidics* **2010**, *4*, 024101.
(23) Sun, P.; Liu, Y.; Sha, J.; Zhang, Z.; Tu, Q.; Chen, P.; Wang, J. *Biosens. Bioelectron.* **2011**, *26*, 1993−1999.
(24) Günberger, A.; Paczia, N.; Probst, C.; Schendzielorz, G.; Eggeling, L.; Noack, S.; Wiechert, W.; Kohlheyer, D. *Lab Chip* **2012**, *12*, 2060−2068.
(25) Unger, M. A.; Chou, H. P.; Thorsen, T.; Scherer, A.; Quake, S. R. *Science* **2000**, *288*, 113−116.
(26) Vyawahare, S.; Griffiths, A. D.; Merten, C. A. *Chem. Biol.* **2010**, *17*, 1052−1065.
(27) Balagadde, F. K.; You, L.; Hansen, C. L.; Arnold, F. H.; Quake, S. R. *Science* **2005**, *309*, 137−140.
(28) Groisman, A.; Lobo, C.; Cho, H.; Campbell, J. K.; Dufour, Y. S.; Stevens, A. M.; Levchenko, A. *Nat. Methods* **2005**, *2*, 685−689.
(29) Lecault, V.; Vaninsberghe, M.; Sekulovic, S.; Knapp, D. J.; Wohrer, S.; Bowden, W.; Viel, F.; McLaughlin, T.; Jarandehei, A.; Miller, M.; Falconnet, D.; White, A. K.; Kent, D. G.; Copley, M. R.; Taghipour, F.; Eaves, C. J.; Humphries, R. K.; Piret, J. M.; Hansen, C. L. *Nat. Methods* **2011**, *8*, 581−586.
(30) Young, E. W.; Beebe, D. J. *Chem. Soc. Rev.* **2010**, *39*, 1036−1048.
(31) Lee, W.; Jambovane, S.; Kim, D.; Hong, J. *Microfluid. Nanofluid.* **2009**, *7*, 431−438.
(32) Jambovane, S.; Duin, E. C.; Kim, S. K.; Hong, J. W. *Anal. Chem.* **2009**, *81*, 3239−3245.
(33) Cook, A.; Lederberg, J. *Genetics* **1962**, *47*, 1335−1353.
(34) Sambrook, J.; Russell, D. W., *Molecular Cloning: A Laboratory Manual*; Cold Spring Harbor Laboratory Press: New York, 2001.
(35) Urbanski, J. P.; Thies, W.; Rhodes, C.; Amarasinghe, S.; Thorsen, T. *Lab Chip* **2006**, *6*, 96−104.
(36) Liu, J.; Hansen, C.; Quake, S. R. *Anal. Chem.* **2003**, *75*, 4718−4723.
(37) Heo, Y. S.; Cabrera, L. M.; Song, J. W.; Futai, N.; Tung, Y. C.; Smith, G. D.; Takayama, S. *Anal. Chem.* **2007**, *79*, 1126−1134.
(38) Reichenbach, H. *Environ. Microbiol.* **1999**, *1*, 15−21.
(39) Paguirigan, A. L.; Beebe, D. J. *Bioessays* **2008**, *30*, 811−821.
(40) Monod, J. *Annu. Rev. Microbiol.* **1949**, *3*, 371−394.
(41) Garau, J.; Gomez, L. *Curr. Opin. Infect. Dis.* **2003**, *16*, 135−143.
(42) Banning, N.; Toze, S.; Mee, B. J. *J. Appl. Microbiol.* **2002**, *93*, 69−76.
(43) Szita, N.; Boccazzi, P.; Zhang, Z.; Boyle, P.; Sinskey, A. J.; Jensen, K. F. *Lab Chip* **2005**, *5*, 819−826.
(44) Lee, H. L. T.; Boccazzi, P.; Ram, R. J.; Sinskey, A. J. *Lab Chip* **2006**, *6*, 1229−1235.
(45) Zuluaga, A. F.; Agudelo, M.; Rodriguez, C. A.; Vesga, O. *BMC Clin. Pharmacol.* **2009**, *9*, 1.
(46) Silva, E.; Diaz, J. A.; Arias, M. J.; Hernandez, A. P.; de la Torre, A. *BMC Clin. Pharmacol.* **2010**, *10*, 3.
(47) Yu, H.; Meyvantsson, I.; Shkel, I. A.; Beebe, D. J. *Lab Chip* **2005**, *5*, 1089−1095.
(48) Raty, S.; Walters, E. M.; Davis, J.; Zeringue, H.; Beebe, D. J.; Rodriguez-Zas, S. L.; Wheeler, M. B. *Lab Chip* **2004**, *4*, 186−190.